Dalton Transactions

PAPER

View Article Online
View Journal | View Issue

Cite this: *Dalton Trans.*, 2014, **43**, 2458

Multi-nuclear silver(I) and copper(I) complexes: a novel bonding mode for bispyridylpyrrolides†

Xiao-Hui Hu, Yan Liang, Chen Li and Xiao-Yi Yi*

Received 7th October 2013,
Accepted 13th November 2013

DOI: 10.1039/c3dt52794h

www.rsc.org/dalton

Reaction of deprotonated 2,5-bis(2′-pyridyl)pyrrole ($HPDP_H$) with AgOTf (where OTf^- = triflato) in THF readily yields a yellow triangular Ag_3 complex $[(PDP_H)Ag]_3$ (**1**), of which the av. Ag···Ag distance is 2.902 Å. A mixture of $HPDP_H$ and AgOTf reacts with PPh_3 to afford a linear Ag_3 complex $[Ag\{(PDP_H)Ag(PPh_3)\}_2]$-(OTf) (**2**·OTf), whereas it reacts with diethyl phosphite in the presence of $Li[N(SiMe_3)_2]$ to yield a di-nuclear complex $Li_2[(PDP_H)Ag_2\{P(O)(OEt)_2\}_2](OTf)$ (Li_2·**3**·OTf). In **2**, the terminal Ag atoms are three co-ordinate containing one phosphorous atom from PPh_3 and two nitrogen atoms of the PDP_H ligand. The center Ag atom is only two coordinate, binding to the residued pyridyl N atom of the PDP_H ligand. In **3**, two silver atoms are bridged by one PDP_H ligand. Treatment of PDP_H with CuCl in the presence of NaH afforded a heterobimetallic copper–sodium complex $[Cu(PDP_H)_2Na(thf)_2]$ (**4**). The PDP_H ligand in **1–4** is nonplanar, with torsion angles between pyridine and pyrrole rings in the range of 15.8–38.3°. The argentophilic interactions, π···π stacking, and weak interaction of Ag···C(aromatic) are observed in these complexes. Interestingly, treatment of the analogous 2,5-bis(6′-bromo-2′-pyridyl)-pyrrole ($HPDP_{Br}$) with AgOTf affords a di-nuclear complex $[(HPDP_{Br})Ag]_2(OTf)_2$ (**5**·$(OTf)_2$). Its $HPDP_{Br}$ ligands coordinate to Ag atoms in a head-to-head fashion, and two protonated pyrrole linkages reside in the anti-parallel direction and are non-coordinating. Short Ag···Br distances of 3.255–3.390 Å are observed.

Introduction

The pincer-like ligand belongs to a type of tridentate ligand where the central anionic or neutral donor site is flanked by two neighboring donor groups.[1,2] It can bind tightly to three adjacent coplanar sites, usually on a transition metal in a meridional configuration. Their metal complexes have attracted interest due to their high stability and ability to catalyze various organic reactions.[3–5] These include the mono-anionic dipyridylpyrrolide (PDP) ligand based on a pyrrole backbone and two pyridine "arms", shown in Scheme 1.[6] The PDP ligand combines the π-backbonding capability of a 18-π electron *N*/*N*/*N* ligand with the flexible π-properties of pyrrolate donors that behave as versatile π-donor and π-acceptor responses to the metal site π-bonding properties. This ligand has been recognized as an analogue of the neutral terpyridine ligand (tpy). In recent years its complexes with late transition metals have received increasing attention. A few opened-shell metals, such as Co(II), Cu(II), Fe(II), Pt(II) and Pd(II), and closed-shell metal of Zn(II) complexes stabilized by dipyridylpyrrolide have been reported.[6–8] All of these complexes display a coplanar mononuclear geometry (mode **I**, Scheme 2), where dipyridylpyrrolide acts as a chelating tridentate ligand binding to the metal center in a meridional configuration. It is noted that the analogous tpy ligand not only acts as a pincer-like ligand to bind to the metal center, but also is capable of aggregating metal ions to form novel multi-nuclear metal complexes. Numerous examples of silver(I) and copper(I) complexes with tpy have been well documented.[9–15] However, the chemistry of a closed-shell d^{10} coinage metal complex containing a bispyridylpyrrolide ligand is still unknown. It inspires us to take more interest in studies aimed at the investigation of silver(I) and copper(I) complexes with PDP ligands and their structural variation.

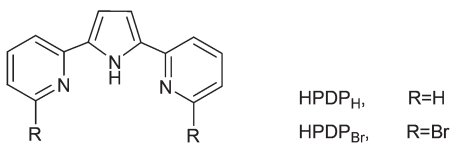

Scheme 1 Structure of dipyridylpyrrolide ligand.

In this paper, we report the syntheses and characterizations of a family of silver(I) and copper(I) complexes stabilized by 2,5-bis(2-pyridyl)pyrrolate ($HPDP_H$) or 2,5-bis(6-bromo-2-pyridyl)pyrrolate ($HPDP_{Br}$) ligands. Complexes **1–4** feature

Key Laboratory of Resources Chemistry of Nonferrous Metals, Ministry of Education, School of Chemistry and Chemical Engineering, Central South University, Changsha, Hunan 410083, P. R. China. E-mail: xyyi@csu.edu.cn; Fax: +86 731 88879616; Tel: +86 731 88879616

†CCDC 963075–963079 for complex **1**, **2**·OTf, Li_2·**3**·OTf, **4** and **5**·$(OTf)_2$, respectively. For crystallographic data in CIF or other electronic format see DOI: 10.1039/c3dt52794h

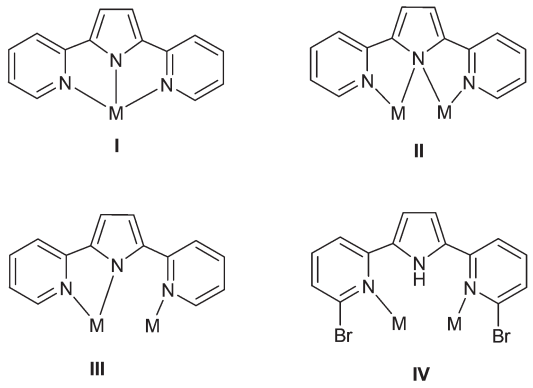

Scheme 2 Coordination modes of bispyridylpyrrolides. κ_3-*N*,*N*′*N*″ (**I**); μ_2-κ_2(*N*,*N*′),κ_2(*N*′,*N*″) (**II**); μ_2-κ_2(*N*,*N*′),*N*″ (**III**); μ_2-*N*′,*N*″ (**IV**).

multi-nuclear metal ions bridged by the twisted PDP_H ligand, and complex **5** displays a novel head-to-head coordination mode of the PDP_{Br} ligand. A novel bonding mode of bispyridylpyrrolide in **1–5** was found.

Experimental

General considerations

All manipulations were carried out under nitrogen by standard Schlenk techniques unless otherwise stated. Solvents were purified, distilled and degassed prior to use. ^{1}H NMR spectra were recorded on a Bruker AV 400 spectrometer operating at 400 MHz, and chemical shifts (δ, ppm) were reported with reference to $SiMe_4$. Infrared spectra (KBr) were recorded on a AVATR360 FT-IR spectrophotometer. The starting 2,5-bis(2′-pyridyl)pyrrolide ($HPDP_H$)[16,17] and 2,5-bis(6′-bromo-2′-pyridyl)-pyrrolide ($HPDP_{Br}$)[18,19] were prepared according to literature methods. All of other chemicals were obtained from J&K Scientific Ltd and used as received.

$[(PDP_H)Ag]_3$ (1)

To a mixture of $HPDP_H$ (33.0 mg, 0.15 mmol) and AgOTf (38.4 mg, 0.15 mmol) in THF (3 mL) was added Et_3N (15.2 mg, 0.15 mmol). The yellow suspension reaction mixture was continued to be stirred for 2 h and filtered. The filtrate was slowly evaporated to give yellow block crystals which were suitable for X-ray diffraction study. The residue yellow solid of **1** was collected, and washed with water, ethanol and Et_2O. Yield: 25.1 mg (51.2%). ^{1}H NMR (d^6-DMSO): δ 8.544 (d, J = 1.2 Hz, 2H), 7.885 (d, J = 3.2 Hz, 2H), 7.802–7.771 (m, 2H), 7.209–7.185 (m, 2H), 6.920 (s, 2H); IR (KBr, cm^{-1}): 3455(w), 3257(m), 1594(s), 1557(m), 1504(m), 1474(s), 1437(s), 1261(vs), 1158(s), 1094(w), 1031(vs), 775(s), 715(w), 636(s), 575(w), 517(m). MS(ESI): *m*/*z* 763.25 (M^+ − PDP_H). Anal. Calcd for $C_{42}H_{30}Ag_3N_9$: C, 51.25; H, 3.07; N, 12.81. Found: C, 51.36; H, 3.35; N, 12.91.

$[Ag\{(PDP_H)Ag(PPh_3)\}_2](OTf)$ (2·OTf)

To a mixture of $HPDP_H$ (33.0 mg, 0.15 mmol) and AgOTf (38.4 mg, 0.15 mmol) in THF (3 mL) was added PPh_3 (39.3 mg, 0.15 mmol). The reaction mixture became clear quickly and was continued to be stirred for 3 h. The filtrate was layered with hexane to give yellow crystals which was suitable for X-ray diffraction study. Yield: 29.5 mg (33.5%). ^{1}H NMR (d^6-DMSO): δ 8.553 (d, J = 2.4 Hz, 4H), 7.888 (d, J = 3.6 Hz, 4H), 7.792 (t, J = 7.6 Hz, 4H), 7.569–7.423 (m, 30H), 7.203 (d, J = 6.0 Hz, 4H), 6.927 (d, J = 0.8 Hz, 4H); ^{31}P NMR ($CDCl_3$): δ 18.30, 14.61 (s, PPh_3). IR (KBr, cm^{-1}): 3446(s), 3257(s), 3048(w), 3003(w), 1590(s), 1557(m), 1516(m), 1476(s), 1460(s), 1437(s), 1260(vs), 1151(s), 1056(s), 1031(vs), 989(m), 948(w), 892(w), 799(m), 774(vs), 714(w), 679(w), 637(s), 617(s), 575(w), 518(m). MS(ESI): *m*/*z* 644.52 (M^+ − OTf + H^+). Anal. Calcd for $C_{65}H_{50}Ag_3F_3N_6O_3P_2S$: C, 54.30; H, 3.51; N, 5.85. Found: C, 53.21; H, 3.68; N, 5.48.

$Li_2[(PDP_H)Ag_2\{P(O)(OEt)_2\}_2](OTf)$ (Li_2·3·OTf)

To a mixture of $HPDP_H$ (33.0 mg, 0.15 mmol) and AgOTf (38.4 mg, 0.15 mmol) in THF (3 mL) was added diethyl phosphite (20.7 mg, 0.15 mmol) and $LiN(SiMe_3)_2$ (0.025 mg, 0.15 mmol). The resulting solution was stirred overnight and filtered. The filtrate was layered with hexane to give yellow crystals which were suitable for X-ray diffraction study. Yield: 21.3 mg (64.5%). ^{1}H NMR ($CDCl_3$): δ 8.599 (d, J = 2.4 Hz, 2H), 7.683–7.674 (m, 4H), 7.104 (d, J = 6.4 Hz, 2H), 6.885 (s, 2H), 3.661 (q, J = 10.0 Hz, 8H), 0.993 (t, J = 6.8 Hz, 12H); ^{31}P NMR ($CDCl_3$): δ 115.17, 108.87 (s, –P(O)$(OEt)_2$). IR (KBr, cm^{-1}): 3444 (br, w), 3068(w), 1588(s), 1556(m), 1502(s), 1449(m), 1426(s), 1326(s), 1252(m), 1148(m), 1042(m), 998(w), 946(w), 922(w), 870(w), 778(m), 746(s), 715(w), 691(w). MS(ESI): *m*/*z* 790.67 (M − LiOTf + H^+). Anal. Calcd for $C_{23}H_{30}Ag_2N_3O_9P_2SF_3Li_2$·$5H_2O$: C, 28.68; H, 4.19; N, 4.36. Found: C, 27.51; H, 3.83; N, 4.28.

$[Cu(PDP_H)_2Na(thf)_2]$ (4)

To a stirred mixture of $HPDP_H$ (132.0 mg, 0.60 mmol) and NaH (14.4 mg, 0.60 mmol) in THF (10 mL) was added CuCl (59.4 mg, 0.6 mmol). The color of the solution changed from yellow to orange immediately. After stirring for 4 h, the suspension solution was filtered. The filtrate was layered by hexane to give darkish red crystals which were suitable for X-ray diffraction study. Yield: 30.5 mg (15% based on PDP ligand). ^{1}H NMR ($CDCl_3$): δ 8.527 (s, 2H), 7.650–7.627 (m, 2H), 7.582 (d, J = 3.6 Hz, 2H), 7.073 (s, 2H), 6.773 (s, 2H), 3.75 (m, 8H), 1.92 (m, 8H); IR (KBr, cm^{-1}): 3435(br, w), 3079(w), 2846(w), 1598(vs), 1556(m), 1509(s), 1455(m), 1432(s), 1335(s), 1260(w), 1154(m), 1057(m), 1012(w), 959(w), 924(w), 790(w), 755(s), 717(w), 644(w). MS(ESI): *m*/*z* 528.00 (M − 2thf + H^+). Anal. Calcd for $C_{36}H_{36}CuN_6NaO_2$: C, 64.42; H, 5.41; N, 12.52. Found: C, 64.25; H, 5.38; N, 12.37.

$[(HPDP_{Br})Ag]_2(OTf)_2$ (5·$(OTf)_2$)

A reaction mixture of $HPDP_{Br}$ (38.0 mg, 0.1 mmol) and AgOTf (25.6 mg, 0.1 mmol) in THF (3 mL) was stirred for 12 h. The

yellow suspension solution was formed and filtered. The filtrate was slowly evaporated to give yellow block crystals which were suitable for X-ray diffraction study. The residue yellow solid of **5**·$(OTf)_2$ was collected and washed with Et_2O. Yield: 34.2 mg (53.5%). ^1H NMR ($CDCl_3$): δ 11.364 (s, 2H), 7.956 (d, J = 3.2 Hz, 4H), 7.752 (t, J = 6.4 Hz, 4H), 7.438 (d, J = 3.2 Hz, 4H), 6.964 (d, J = 0.4 Hz, 4H). IR (KBr, cm^{-1}): 3440(br, w), 3340(w), 3241(w), 3107(w), 1587(s), 1541(s), 1432(vs), 1389(w), 1252(vs), 1163(vs), 1129(m), 1109(m), 1081(m), 1056(w), 998(m), 787(s), 754(m), 633(s), 573(m), 516(m). MS(ESI): m/z 487.08 (M^{2+} − 2OTf). Anal. Calcd for $C_{15}H_9AgBr_2F_3N_3O_3S{\cdot}2H_2O$: C, 26.81; H, 1.95; N, 6.25. Found: C, 26.51; H, 1.92; N, 6.10.

X-Ray crystallography

Diffraction data of **1**, **2**·OTf, Li_2·**3**·OTf, **4**·2(thf), **5**·$(OTf)_2$ were recorded on a Bruker CCD diffractometer with monochromatized MoK radiation (λ = 0.71073 Å). Data collection and reduction were carried out using SAINT and CrysAlisPro program. SADABS was used for the absorption correction.[20] Structures were solved by direct methods and refined by full-matrix least-squares on F^2 using the SHELXTL software package.[21] Atomic positions of non-hydrogen atoms were refined with anisotropic parameters. All hydrogen atoms were introduced at their geometric positions and refined as riding atoms. In anionic **3**, C21, C22 atoms on diethyl phosphite are disordered with 65/35 occupancy. The co-crystallized THF solvent is found to be disordered, and has been refined with an occupancy of 53/47.

Results and discussion

Synthesis and characterization

Treatment of AgOTf with one equivalent of $HPDP_H$ in the presence of a base, such as Et_3N, affords yellow precipitate in medium yield (Scheme 3). This reaction becomes completed within less than 1 h at room temperature. The isolated solid is identified as tri-nuclear $[(PDP_H)Ag]_3$ (**1**) by NMR spectrum. **1** is insoluble in common organic solvent, but soluble in the polar solvent such as DMF and DMSO. Upon reaction of a mixture of AgOTf and $HPDP_H$ with phosphine, the silver phosphine complexes are formed. As illustrated in Scheme 3, the suspension mixture of AgOTf and $HPDP_H$ reacts with one equivalent of PPh_3 to produce yellow tri-nuclear $[Ag\{(PDP_H)Ag(PPh_3)\}_2](OTf)$ (**2**·OTf), whereas it reacts with one equivalent of diethyl phosphite in the presence of $LiN(SiMe_3)_2$ to afford yellow di-nuclear $Li_2[(PDP_H)Ag_2\{P(O)(OEt)_2\}_2](OTf)$ (Li_2·**3**·OTf). Complexes of **2**·OTf and Li_2·**3**·OTf are soluble in THF, CH_2Cl_2, while insoluble in Et_2O and hexane. Attempts to produce other phosphine complexes by treatment of the mixture of AgOTf and $HPDP_H$ with 1,2-bis(diphenylphosphino), 1,10-dilhydro-9-oxa-10-phosphaphenanthrene 10-oxide have failed. Treatment of CuCl with $HPDP_H$ in the presence of Et_3N gives a red intractable oily product. NaH instead of Et_3N used to deprotonate the $HPDP_H$, copper–sodium heterobimetallic complex $[Cu(PDP_H)_2Na(thf)_2]$ (**4**) is isolated. Di-nuclear $[(HPDP_{Br})Ag]_2(OTf)_2$ (**5**·$(OTf)_2$) is synthesized by the treatment of AgOTf with one equivalent of $HPDP_{Br}$ in THF.

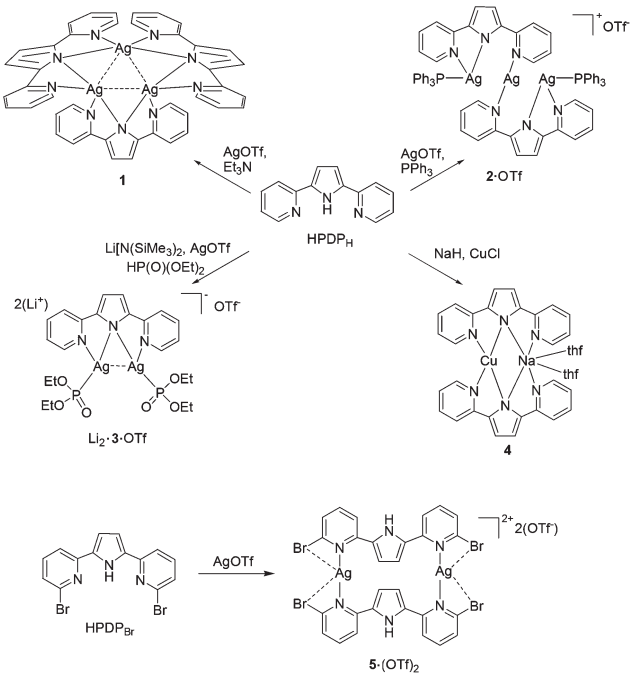

Scheme 3 Syntheses of complexes **1**, **2**·OTf, Li_2·**3**·OTf, **4** and **5**·$(OTf)_2$.

Complexes **1**, **2**·OTf, Li_2·**3**·OTf, **4** and **5**·$(OTf)_2$ are characterized by IR, NMR spectra and X-ray diffraction study. The IR spectra are recorded in the region 4000–450 cm^{-1} on KBr disks. The PDP_H ligand has several distinctive signals, including the weak aromatic C–H stretching at 2976–3107 cm^{-1}. A region from 1420 to 1590 cm^{-1} consists of three or four quite intense signals, corresponding to the in-plane vibrations of the C=C bonds. All of the above are presented in these five complexes. In addition, **2**·OTf, Li_2·**3**·OTf, and **5**·$(OTf)_2$ show a strong stretching band at 1253–1278 cm^{-1} due to the triflato group. The ^1H NMR spectrum of **1** in d^6-DMSO clearly reveals the formation of the Ag–N(pyrrolate) bond, which is indicated by the absence of the imino N–H resonance. Of the four chemical shifts (δ = 8.55, 7.88, 7.78 and 7.20 ppm) for the pyridyl ring hydrogens, the most downfield resonance (δ = 8.55 ppm) is routinely assigned to the H *ortho* to the nitrogen. The proton resonances of the pyrrole ring appear at 6.92 ppm as a doublet. The ^1H NMR spectrum of pyridine and pyrrole protons in **2**·OTf, Li_2·**3**·OTf and **4** in $CDCl_3$ closely resemble those in **1**. The $^{31}P\{^1H\}$ NMR spectra of **2**·OTf and Li_2·**3**·OTf display multiple peaks of 18.3, 14.6 ppm and 115.2, 108.9 ppm attributable to PPh_3 and $P(O)(OEt)_2$ ligands, respectively. In the ^1H NMR spectrum of **5**·$(OTf)_2$, a resonance of 11.36 ppm is observed, tentatively assigned to the imino proton on the pyrrole ring, which is consistent with the solid state structure.

Description of structure

A summary of the crystallographic data and experimental details for these five complexes are selected in Table 1.

Table 1 Crystallographic data and experimental details for **1**, **2**·OTf and Li_2·**3**·OTf, **4** and **5**·$(OTf)_2$

Complexes	**1**	**2**·OTf	Li_2·**3**·OTf	**4**	**5**·$(OTf)_2$
Formula	$C_{42}H_{30}Ag_3N_9$	$C_{65}H_{50}Ag_3F_3N_6O_3P_2S$	$C_{54}H_{76}Ag_4F_6Li_4N_6O_{20}P_4S_2$	$C_{36}H_{36}CuN_6NaO_2$	$C_{30}H_{18}Ag_2Br_4F_6N_6O_6S_2$
Fw	984.36	1437.72	1890.45	671.24	1272
Crystal system	Monoclinic	Monoclinic	Triclinic	Orthorhombic	Triclinic
Space group	*Cc*	*C*2/*c*	$P\bar{1}$	*Fdd*2	$P\bar{1}$
a (Å)	15.055(3)	19.8842(3)	12.4463(2)	11.6882(3)	7.8073(16)
b (Å)	19.328(4)	17.3938(3)	12.9013(2)	30.6434(8)	15.310(3)
c (Å)	12.632(2)	17.4070(2)	14.0856(2)	18.0484(5)	16.630(3)
α (°)	90	90	66.1580(10)	90	110.57(3)
β (°)	104.687(2)	108.2390(10)	69.5560(10)	90	98.30(3)
γ (°)	90	90	74.9330(10)	90	96.19(3)
V (Å^3)	3555.6(11)	5717.94(15)	1919.76(5)	6464.3(3)	1814.4(6)
Z	4	4	1	8	2
ρ_{calc} (g cm^{-3})	1.839	1.670	1.635	1.379	2.328
T (K)	296(2)	120(2)	296(2)	120(2)	120(2)
μ (mm^{-1})	1.683	1.174	1.224	0.732	5.684
No. of refln.	9592	29 949	22 224	7241	15 452
No. of indep. refln.	4730	6557	7469	2976	8113
R_{int}	0.0561	0.0180	0.0163	0.0137	0.0211
GoF	0.975	1.024	1.010	1.049	1.059
R_1, wR_2 [$I > 2\sigma(I)$]	0.0506, 0.1118	0.0205, 0.0671	0.0361, 0.1047	0.0178, 0.0530	0.0266, 0.0585
R_1, wR_2 (all data)	0.0644, 0.1212	0.0257, 0.0793	0.0459, 0.1141	0.0180, 0.0532	0.0355, 0.0679

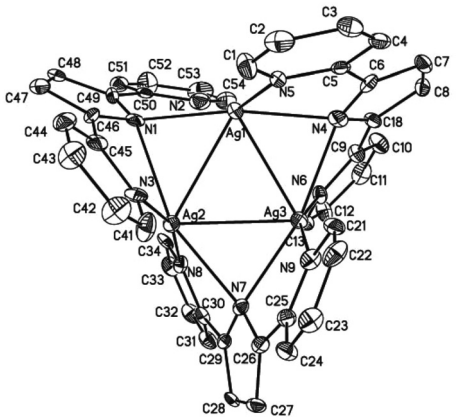

Fig. 1 ORTEP diagram of trinuclear Ag(I) complex **1** with ellipsoids shown at the 50% probability level. The hydrogen atoms are omitted for clarity. Selected bond distances (Å): Ag1–Ag2 2.9370(12), Ag1–Ag3 2.8732(13), Ag2–Ag3 2.8937(13), Ag1–N1 2.281(9), Ag1–N2 2.659(9), Ag1–N4 2.333(11), Ag1–N5 2.468(10), Ag2–N1 2.494(9), Ag2–N3 2.310(9), Ag2–N7 2.455(10), Ag2–N8 2.283(10), Ag3–N4 2.464(11), Ag3–N6 2.361(9), Ag3–N7 2.369(11), Ag3–N9 2.368(9); selected bond angles (°): Ag2–Ag1–Ag3 59.73(3), Ag1–Ag2–Ag3 59.04(3), Ag1–Ag3–Ag2 61.23(3), Ag1–N1–Ag2 75.8(2), Ag1–N4–Ag3 73.5(3), Ag2–N7–Ag3 73.7(3), N1–Ag1–N4 169.4(4), N1–Ag1–N5 115.3(3), N4–Ag1–N5 71.2(3), N8–Ag2–N3 163.8(4), N8–Ag2–N7 71.9(3), N3–Ag2–N1 71.3(3), N7–Ag2–N1 159.4(3), N6–Ag3–N9 161.3(3), N6–Ag3–N4 70.6(3), N9–Ag3–N7 71.4(3), N7–Ag3–N4 166.2(3).

Complex **1** is non-centrosymmetric and crystallizes in the monoclinic space group *Cc*. As shown in Fig. 1, a nearly equilateral triangle Ag_3 core (Ag2–Ag1–Ag3 59.73(3)°, Ag1–Ag2–Ag3 59.04(3)°, Ag1–Ag3–Ag2 61.23(3)°) is supported by three PDP_H ligands in the μ_2-(κ_2-*N*,*N*′),(κ_2-*N*,*N*″) (**II**) bonding mode (Scheme 2). This core structure is quite similar to those of Ag_3 N-heterocyclic carbene complexes, $[Ag_3(CH_3im(CH_2py))_3(NCCH_3)_2]^{3-}$, $[Ag_3(im(CH_2py)_2)_3]^{3-}$ and $[Ag_3(im(CH_2Mepy)_2)_3]^{3-}$,[22,23] and Cu_3 monopyridylpyrrole complex.[24,25] Short Ag–Ag distances in **1** (Ag1–Ag2 2.9370(12) Å, Ag1–Ag3 2.8732(13) Å, Ag2–Ag3 2.8937(13) Å) due to the silver–silver interaction are slightly longer than av. 2.784 Å observed in Ag_3 N-heterocyclic carbene complexes.[22] The Ag–N distances in **1** range from 2.281(9) to 2.659(3) Å. To be noticeable, the Ag1–N2(pyridine) bond (2.659(3) Å) is significantly longer than other Ag–N bonds in **1**, indicating that there may be no or only a weak interaction between Ag1 and N2. This is consistent with the non-centrosymmetric structure of complex **1**. Thus, the Ag1 atom is three coordinate, while Ag2 and Ag3 atoms are four coordinate in distorted tetrahedron geometry.

Complex **2**·OTf crystallizes in the monoclinic space group *C*2/*c*. The structure of **2** is shown in Fig. 2. A trisilver helicate is present with the Ag···Ag distance of 3.12827(14) Å; the μ_2-(κ_2-*N*,*N*′),*N*″ (**III**) bonding mode of the PDP_H ligand occurs. The terminal Ag1 and Ag1A atoms are three coordinate and bond to two nitrogen donors of the ligand and one triphenylphosphine; the coordination geometry is Y-shape with larger N1–Ag1–P1 (132.85(4)°), N2–Ag1–P1 (148.77(4)°) and smaller N1–Ag1–N2 (74.28(6)°) bond angles. The central Ag2 silver atom is only two coordinate with short Ag–N bonds (2.1275(16) Å) to terminal pyridine rings of each of two ligands and two longer Ag···N contacts to the central pyrrole ring (2.89 Å).

Diethyl phosphite instead of PPh_3 is added into a mixture of $HPDP_H$ and AgOTf in the presence of $Li[N(SiMe_3)_2]$ to produce binuclear Li_2·**3**·OTf. As shown in Fig. 3, PDP_H ligand adopts mode **II** to coordinate two silver atoms. Each silver atom is tri-coordinated by two N atoms from PDP_H ligand and one P atom from diethyl phosphite. Here, the Ag–N(pyrrole) distance (av. 2.437 Å) is longer than that of Ag–N(pyridine) (av. 2.231 Å). The two silver atoms have a distance of 2.8282(9) Å indicating a strong Ag···Ag interaction, which is comparable with the Ag–Ag distance found previously. Lithium triflate is cocrystallized in Li_2·**3**·OTf. Its lithium cations are surrounded

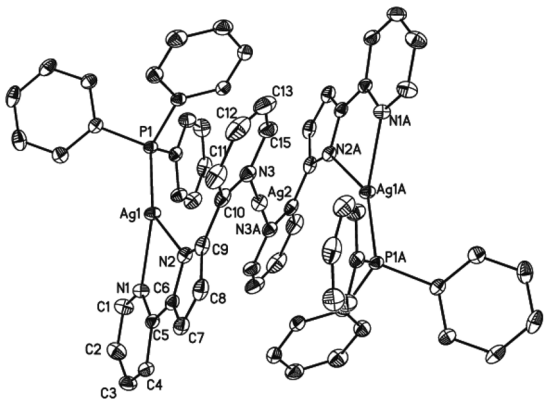

Fig. 2 ORTEP diagram of trinuclear Ag(I) cationic **2** with ellipsoids shown at the 50% probability level. The hydrogen atoms are omitted for clarity. Selected bond distances (Å): Ag1–N1 2.3645(16), Ag1–N2 2.2163(15), Ag1–P1 2.3503(5), Ag2–N3 2.1275(16), Ag1–Ag2 3.12827(14); selected bond angles (°): N1–Ag1–P1 132.85(4), N2–Ag1–P1 148.77(4), N1–Ag1–N2 74.28(6), N3–Ag2–N3A 180.00(6), Ag1–Ag2–Ag1A 180.000(3). Symmetry transformations used to generate equivalent atoms: A $-x + 1, -y + 1, -z$.

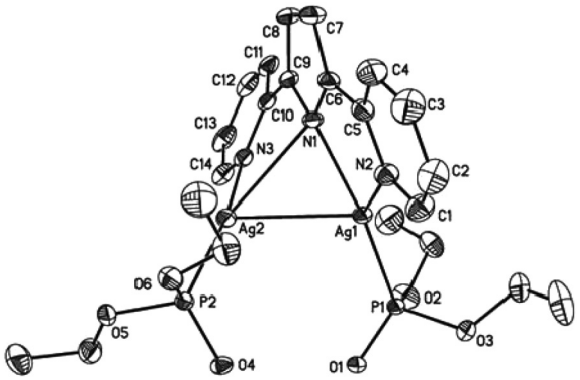

Fig. 3 ORTEP diagram of dinuclear Ag(I) anionic **3** with ellipsoids shown at the 50% probability level. The hydrogen atoms are omitted for clarity. Selected bond distances (Å): Ag1–N1 2.402(7), Ag1–N2 2.226(8), Ag1–P1 2.325(2), Ag2–N1 2.471(7), Ag2–N3 2.235(8), Ag2–P2 2.316(3), Ag1–Ag2 2.8181(9); selected bond angles (°): N2–Ag1–P1 146.18(19), N2–Ag1–N1 74.1(3), P1–Ag1–N1 139.28(18), N3–Ag2–P2 149.0(2), N3–Ag2–N1 74.3(3), P2–Ag2–N1 135.78(18).

by oxygen atoms from tetrahydrofunan, diethylphosphite and/or the triflato ligand (Fig. 4), resulting in the formation of a tetranuclear ladder-like structure. Li2 and Li2A atoms are four coordinate in tetrahedron geometry with an average Li–O bond distance of 1.943 Å. Li1 and Li1A atoms are coordinated by five oxygen atoms to form a distorted bipyramidal geometry, if longer Li–O bond (Li1–O1A 2.395(7) Å, Li1–O2A 2.299(8) Å) could not be ignored.

In complex **4**, a helical arrangement around the copper(I) and sodium ions is displayed in Fig. 5. Copper(I) atom is chelate-bound by both PDP_H ligands with two nitrogen atoms, while sodium rises to hexa-coordination, additionally bound to two tetrahydrofuran solvent molecules. Within this structural arrangement, the central pyrrole nitrogen atoms N1 and

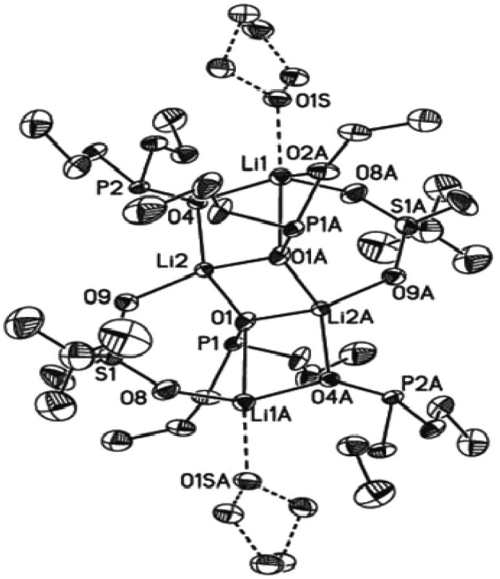

Fig. 4 Coordination geometry of lithium cationic in Li_2·**3**·OTf. Selected bond distances (Å): Li1–O4 1.961(8), Li1–O8A 1.943(8), Li1–O1S 1.935(18), Li1–O1A 2.395(7), Li1–O2A 2.299(8), Li2–O1 1.954(7), Li2–O4 1.933(6), Li2–O9 1.948(6), Li2–O1A 1.939(6).

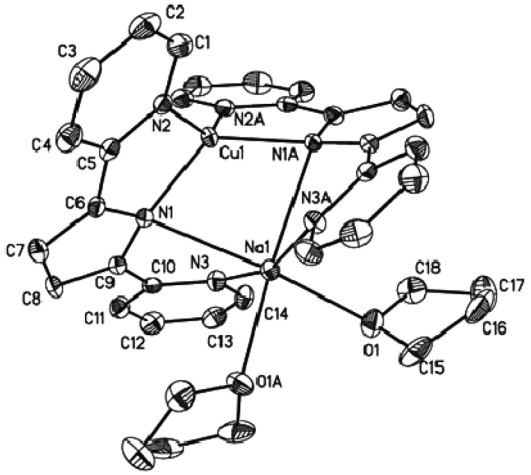

Fig. 5 ORTEP diagram of copper(I) complex **4** with ellipsoids shown at the 50% probability level. The hydrogen atoms are omitted for clarity. Selected bond distances (Å): Cu(1)–N(1) 2.0581(12), Cu(1)–N(2) 2.0041(12), Na(1)–N(1) 2.6745(13), Na(1)–N(3) 2.4365(12), Na(1)–O(1) 2.3736(13), Cu(1)–Na(1) 2.8927(9). Selected bond angles (°): N1–Cu1–N2 82.61(5), N1–Cu1–N2A, 116.04(5), N1–Cu1–N1A 125.52(7), N2–Cu1–N2A 140.35(7).

N1A are μ-bridged Cu1 and Na1 with Cu1–N1 and Na1–N1 distances of 2.0581(12) and 2.6745(13) Å, respectively. The Na1–N (pyridine) and Na1–O(thf) bond distances are 2.4365(12) and 2.3736(13) Å, respectively (Fig. 5).

The silver(I) complex supported by the bromo-substituted PDP_{Br} ligand is also studied. Complex **5**·$(OTf)_2$ crystallizes in the triclinic space group $P\bar{1}$ with an asymmetric unit containing two one-half of cationic **5** and two OTf^- anions (Fig. 6). X-ray dif-fraction studies reveal that the PDP_{Br} ligands coordinate to

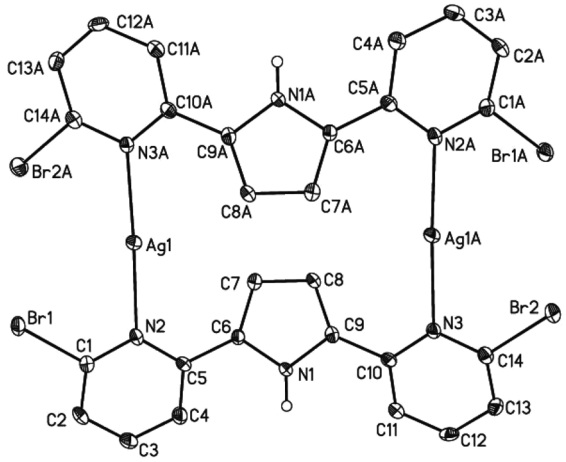

Fig. 6 ORTEP diagram of dinuclear Ag(I) cationic **5** with ellipsoids shown at the 50% probability level. The hydrogen atoms are omitted for clarity except of the pyrrole proton on the nitrogen atom. Selected bond distances (Å): Ag1–N2 2.282(3), Ag1–N3A 2.276(3), Ag3–N23 2.260(3), Ag3–N22B 2.246(3); selected bond angles (°): N3A–Ag1–N2 177.30(9), N22B–Ag3–N23 173.72(9). Symmetry transformations used to generate equivalent atoms: A $-x+1, -y, -z$; B $-x, -y, -z+1$.

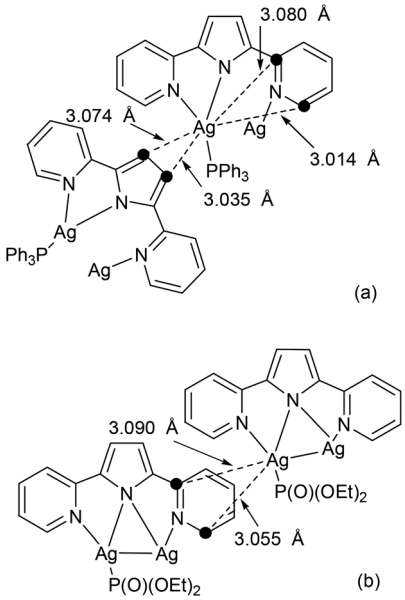

Scheme 4 (a) Ag···C contact in **2**·OTf; (b) Ag···C contact in Li_2·**3**·OTf; (c) Ag···Br contact in **5**·$(OTf)_2$.

Ag atoms only with pyridine nitrogen in a head-to-head fashion (mode **IV**). The central pyrrole is protonated and non-coordinated, residing in the anti-parallel direction. To our knowledge, this is the first report of such a coordination mode of the bispyridylpyrrolide ligand. The Ag–N bond distances (2.246(3)–2.282(3) Å) are comparable with those for the Ag–N-(pyridine) complexes. The N–Ag–N bond angles are almost linear (N3A–Ag1–N2 177.30(9) and N22B–Ag3–N23 173.72(9)°).

All known bispyridylpyrrolide metal complexes, such as $[Co(PDP_H)_2]$, $[M(PDP_H)Cl]$ (M = Pd, Pt),[7,8] are mononuclear and rigorously planar, including the coplanarity of the three rings of the bispyridylpyrrolides. In comparison, the most noteworthy feature of the structures in this paper is the aggregation of the coinage metal by nonplanar bispyridylpyrrolides. The two side rings and the pyrrole ring of the ligand have twisted to form three interplanar angles with the central ring, which are in the range of 15.8–38.3°, well comparable with those found in the coinage metal terpyridine complexes.[10–15]

Potential weak interactions, such as π–π stacking, Ag···C-(aromatic) and/or Ag···Br interactions are extensively observed in **1–5**. Weak intermolecular face-to-face π–π stacking is found within the two pendant pyridyls (centroid–centroid distance 3.7957 and 3.8587 Å for **1**, 3.7985, 3.7760 Å for **2**·OTf and 3.901 Å for Li_2·**3**·OTf, 3.734 Å for **5**).

Silver is known to have a remarkable high affinity for some aromatic π-donor system. As shown in Scheme 4, the aromatics in **2**·OTf and Li_2·**3**·OTf are found η^2-interacting with the silver ions. The separations vary in the range of 3.01–3.13 Å, and the next closest contacts between Ag and C/N are all over 3.3 Å, which is well comparable with those for polycyclic aromatic silver(I) compounds.[26] In the case of **2**·OTf, only terminal Ag is involved in the Ag···C contacts. The contact between Ag and N on the sideway pyridine ring is short (3.080 and 3.014 Å). That could be a cause of the ligand twisting and forming a large torsion angle of 38.3° between the pyrrole and sideways pyridine rings. The intermolecular contact is perpendicular to the coordination plane of NNP, possibly causing the Ag to be out of this plane by 0.21 Å. The similar intermolecular contact (3.090 Å, 3.055 Å) in Li_2·**3**·OTf is observed, which is in the opposite direction of Ag···Ag contact. In the case of **5**·$(OTf)_2$, the strong affinity of the "soft" bromine toward silver atom proves to be very effective in adjusting the coordination framework.[27] The distances between silver and the adjacent Br atom within one molecule, such as Ag1···Br3 (3.390 Å), Ag1···Br4 (3.248 Å), Ag2···Br1 (3.253 Å), Ag2···Br2 (3.239 Å), are shorter than their van der Waals radius, which is analogous to that in the silver complex of *N*-4-bromophenyl-*N*-4-pyridylurea (3.261 Å).[27a] PDP_{Br} could hinder the aggregation of silver atoms, perhaps due to the weak steric effect of the *ortho*-bromine atom. Thus, the combination of Ag···Br contacts and steric hindrance of Br in **5** may lead PDP_{Br} in the formation of mode **IV**, although the PDP ligand favorable for forming other chelating bonding modes, such as **I**, **II** and **III**.

Conclusion

In summary, we have successfully designed and synthesized silver(I) and copper(I)-bispyridylpyrrolide complexes with different nuclearity. Structural investigation reveals that the bispyridylpyrrolide ligand has analogous chemistry to terpyridine, being capable of aggregating metal ions to form novel multi-nuclear metal complexes. PDP_H in **1–4** acts as a bridging ligand to coordinate two metal atoms in bonding modes **II** and **III**, while PDP_{Br} in **5** binds to silver atoms in a face-to-face fashion (bonding mode **IV**). It seems likely that the bonding

flexibility of the central pyrrole nitrogen and the range of potential molecular interactions, such as π–π stacking, Ag···Br, Ag···C interactions, directly lead the bispyridylpyrrolide ligand to change its bonding mode, and to rotate away from planarity to accommodate a bridging structural role.

Acknowledgements

This work was supported by the National Natural Science Foundation of China (project 21001118), China Postdoctoral Science Foundation (2011M500129) and the Postdoctoral Science Foundation of Central South University. This material is available free of charge *via* the Internet at http://pubs.acs.org.

Notes and references

1 C. J. Moulton and B. L. Shaw, *J. Chem. Soc., Dalton Trans.*, 1976, 1020–1024.
2 J. Dehand and M. Pfeffer, *Coord. Chem. Rev.*, 1976, **18**, 327–352.
3 M. E. van der Boom and D. Milstein, *Chem. Rev.*, 2003, **103**, 1759–1792.
4 M. G. Scheibel, B. Askevold, F. W. Heinemann, E. J. Reijerse, B. de Bruin and S. Schneider, *Nat. Chem.*, 2012, **4**, 552–558.
5 N. Selander and K. J. Szabó, *Chem. Rev.*, 2011, **111**, 2048–2076.
6 J. W. Ciszek, Z. K. Keane, L. Cheng, M. P. Stewart, L. H. Yu, D. Natelson and J. M. Tour, *J. Am. Chem. Soc.*, 2006, **128**, 3179–3189.
7 G. H. Imler, Z. Lu, K. A. Kistler, P. J. Carroll, B. B. Wayland and M. J. Zdilla, *Inorg. Chem.*, 2012, **51**, 10122–10128.
8 F. Hein and U. Beierlein, *Pharm. Zentralhalle Dtschl.*, 1957, **96**, 401–421.
9 M. Al-Anber, B. Walfort, S. Vatsadze and H. Lang, *Inorg. Chem. Commun.*, 2004, **7**, 799–802.
10 Y. Cui and C. He, *J. Am. Chem. Soc.*, 2003, **125**, 16202–16203.
11 G. Baum, E. C. Constable, D. Fenske, C. E. Housecroft and T. Kulke, *Chem. Commun.*, 1998, 2659–2660.
12 E. C. Constable, T. Kulke, M. Neuburger and M. Zehnder, *Chem. Commun.*, 1997, 489–490.
13 Effendy, F. Marchetti, C. Pettinari, R. Pettinari, B. W. Skelton and A. H. White, *Inorg. Chim. Acta*, 2007, **360**, 1414–1423.
14 (*a*) H. Feng, X.-P. Zhou, T. Wu, D. Li, Y.-G. Yin and S. W. Ng, *Inorg. Chim. Acta*, 2006, **359**, 4027–4035; (*b*) Z. Ma, Y.-P. Xing, M. Yang, M. Hu, B.-Q. Liu, M. F. C. G. da Silva and A. J. L. Pombeiro, *Inorg. Chim. Acta*, 2009, **362**, 2921–2926.
15 M. J. Hannon, C. L. Painting, E. A. Plummer, L. J. Childs and N. W. Alcock, *Chem.–Eur. J.*, 2002, **8**, 2225–2238.
16 H. Schindlbauer, *Monatsh. Chem.*, 1968, **99**, 1799–1807.
17 R. A. Jones, M. Karatza, T. N. Voro, P. U. Civcir, A. Franck, O. Ozturk, J. P. Seaman, A. P. Whitmore and D. J. Williamson, *Tetrahedron*, 1996, **52**, 8707–8724.
18 D. C. Owsley, J. M. Nelke and J. J. Bloomfield, *J. Org. Chem.*, 1973, **38**, 901–903.
19 Z. Zhang, J. M. Lim, M. Ishida, V. V. Roznyatovskiy, V. M. Lynch, H.-Y. Gong, X. Yang, D. Kim and J. L. Sessler, *J. Am. Chem. Soc.*, 2012, **134**, 4076–4079.
20 G. M. Sheldrick, *SADABS*, University of Göttingen, Germany, 1997.
21 G. M. Sheldrick, *SHELXTL-Plus V5.1 Software Reference Manual*, Bruker AXS Inc., Madison, Wisconsin, USA, 1997.
22 (*a*) V. J. Catalano and S. J. Horner, *Inorg. Chem.*, 2003, **42**, 8430–8438; (*b*) V. J. Catalano and M. A. Malwitz, *Inorg. Chem.*, 2003, **42**, 5483–5485; (*c*) V. J. Catalano and A. L. Moore, *Inorg. Chem.*, 2005, **44**, 6558–6566.
23 (*a*) P. A. Leach, S. J. Geib and N. J. Cooper, *Organometallics*, 1992, **11**, 4367–4370; (*b*) J. C. Garrison, C. A. Tessier and W. J. Youngs, *J. Organomet. Chem.*, 2005, **690**, 6008–6020.
24 V. J. Catalano, L. B. Munro, C. E. Strasser and A. F. Samin, *Inorg. Chem.*, 2011, **50**, 8465–8476.
25 J. G. Andino, J. A. Flores, J. A. Karty, J. P. Massa, H. Park, N. P. Tsvetkov, R. J. Wolfe and K. G. Caulton, *Inorg. Chem.*, 2010, **49**, 7626–7628.
26 M. Munakata, L.-P. Wu, G.-L. Ning, T. Kuroda-Sowa, M. Maekawa, Y. Suenaga and N. Maeno, *J. Am. Chem. Soc.*, 1999, **121**, 4968–4976.
27 (*a*) S. K. Chandran, R. Thakuria and A. Nangia, *CrystEngComm*, 2008, **10**, 1891–1898; (*b*) M. D. Ward, S. M. Couchman and J. C. Jeffery, *Acta Crystallogr., Sect. C: Cryst. Struct. Commun.*, 1998, **54**, 1820–1823.

